

Supporting Information for

Monitoring the neurotransmitter release of human midbrain organoids using a redox cycling microsensor array as a novel tool for personalized Parkinson's disease modeling and drug testing

Cristian Zanetti[‡], Sarah Spitz^{‡,§}, Emanuel Berger[†], Silvia Bolognin[†], Lisa Smits[†], Mario Rothbauer^{‡1}, Philipp Crepaz[‡], Julie Rosser^{‡2}, Martina Marchetti-Deschmann[‡], Jens C. Schwamborn[†] and Peter Ertl^{‡*}

[‡] Faculty of Technical Chemistry, Vienna University of Technology (TUW), Getreidemarkt 9/164, 1060 Vienna, Austria

[†] Developmental and Cellular Biology, Luxembourg Centre for Systems Biomedicine (LCSB), University of Luxembourg, 7 avenue des Hauts-Fourneaux, 4362 Esch-sur-Alzette, Luxembourg).

* corresponding author: Peter Ertl, peter.ertl@tuwien.ac.at

Keywords: Dopamine, Parkinson disease, redox-cycling, electrochemistry, iPSC, midbrain organoid, MPA, LC-MRM-MS

¹ Current address: Medical University Vienna, Austria

² Current address: Pregenerate Inc., Vienna, Austria

Table of Contents

Electrochemistry

Figure S1. 10-minutes redox cycling signals of 5 μM DA in PBS, for both MPA and control sensors. The signal drift was calculated with a linear fit between 110 s and 600 s. The MPA effect on the signal drift was evaluated by comparing the slopes from the linear fits, see Table below for details.	3
Table S1. Results of the signal drift calculation from the 10-minutes redox cycling experiment. The linear fit results were averaged ($n = 2$) and are displayed in the table with the correlated standard error and the slope in degrees. The effect of MPA at the generator removed the signal drift (the value marked with an asterisk was not significantly different from zero). The MPA effect on the collector (cathodic currents) significantly reduced drift of signal from a positive (decreasing signal) slope to a slightly negative value (increasing signal over time), overall this shows a positive impact of MPA on the signal stability.	3
Figure S2. Optimization of the generator potential. On the top: Chronoamperometric responses of DA and AA at the sensor with increasing generator electrode potentials. The potential was stepped every 30 s from 0 to +0.30 V, the collector potential was set to -0.1 V. On the bottom: ratio of the recorded DA and AA signals. The experiment was performed in PBS (pH = 7.4).	4
Figure S3. Optimization of the collector potential. On the top: chronoamperometric responses of DA and AA at the sensor with decreasing collector electrode potentials. The potential was stepped every 30 s from 0 to -0.20 V, the generator potential was set to +0.25 V. On the bottom: ratio of the recorded DA and AA signals. The experiment was performed in PBS (pH = 7.4).	4
Figure S4. Generator and Collector signals of ascorbic acid (AA) and dopamine (DA) solutions in PBS at MPA modified sensor. a) At the generator the DA signal is higher than the AA signal, and when the two components are mixed in the same solution the resulting signal is higher than the sum of the separate ones, this synergic action is attributed to AA reducing DA-quinone, thus increasing diffusion gradients and leading to higher currents; b) at the collector the AA signal is silent, while the DA signal is visible (due to reduction of DA-quinone), the copresence of DA and AA in solution leads to a silent signal, this is also attributed to AA reducing DA-quinone.	5
Table S2. Sensor intra-batch and inter-batch repeatability. Each sensitivity measurement was obtained from the slope of a 0-1000 nM DA calibration curve in PBS.	6
Figure S5. Time resolved monitoring of DA sensitivity of the sensor ($n = 4$) to assess sensor stability. The slope of the linear regression was not significantly different from zero ($\alpha = 0.05$).	6
Table S3. Long-term stability study. DA signal was measured on the month of manufacturing and also after 20 months ($n = 3$). Selectivity towards AA was also measured after 20 months.	6
Table S4. Detailed Results of the analysis of selectivities to DA change after MPA modification. The selectivity was calculated as the ratio of the biomolecule signal (nC/nM) and the DA signal (nC/nM). The percent change represents the change in selectivity to DA after MPA modification. Not detected or n.a.: the signal of the compound was not significantly different from the background (PBS, $\alpha = 0.05$, two-tailed t test).	7
Figure S6. Electrochemical sensor calibration of DA in both PBS and cell culture medium. Generator (Gen.) signals include PBS (open squares) and cell culture medium (open circles). Collector (Coll.) signals include PBS (up open triangles) and cell culture medium (down open triangles). Linear regressions equations are visible. Error bars: standard error of the mean.	7
Table S5. Detailed results of the linear regression of DA calibration in PBS and cell culture medium. The LOD was calculated as the value of the blank (cultivated cell culture medium) plus three times the error of the blank (SEM). The lowest limit of the linear range is the adjusted to be \geq LOD.	7

LC-MRM-MS

Table S6. Elution program of the LC-MRM-MS method using 0.1 % aqueous formic acid as eluent A and acetonitrile as eluent B.	8
Figure S7. LC-MRM-MS chromatograms showing chromatographic performance for the most intense MRM transitions. A) Injection of an aqueous mixture of standards (on column: 19.3 pmol GABA, 2.5 pmol norepinephrine (NE), 3.1 pmol epinephrine (EP), 3.7 pmol L-DOPA, 4.0 pmol dopamine (DA), 9.1 pmol DOPAC); B) Chromatogram of the healthy organoid line sample at day 60. EP and NEP had a S/N < 3.	8
Table S8. Limits of Detection (LOD) and Limits of Quantitation (LOQ) obtained for 6 neurotransmitters measured from cell culture medium after minimal sample preparation by LC-MRM-MS. 5 μ l injections. LOD: S/N > 3, LOQ: S/N > 10.	9
Table S9. Summary of intraday reproducibility for the LC-MRM-MS analysis of neurotransmitters measured directly from cell culture medium after minimal sample preparation. On the left column averaged coefficient of variation (CV) values of four different human midbrain organoid supernatant (differentiation day 60), N/A: data not available (S/N < 3); On the right column averaged CV values of five different standard dilutions (S/N > 10, same data as Table 3 in the manuscript). Every injection was done thrice.	9

Cell Culture and Immunohistochemistry

Table S10. hMO lines description with references.	10
Figure S8. Immunohistochemical staining of an hMO at day 53 of differentiation. The staining reveals tyrosine hydroxylase (TH, red) positive dopaminergic neurons ((a) and (b)) as well as the neuronal marker TUJ1 (green) and DAPI stained nuclei (blue) (a).	10

Electrochemistry

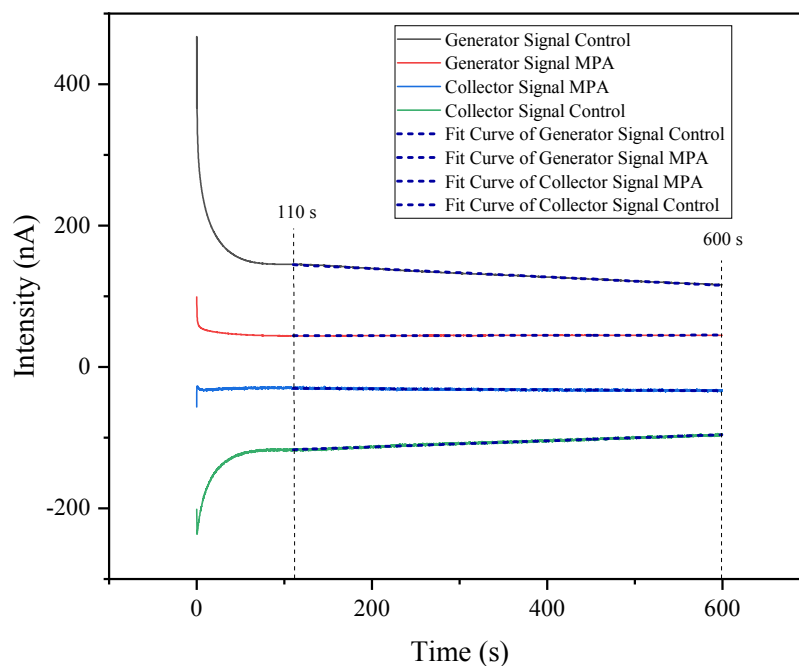


Figure S1. 10-minutes redox cycling signals of 5 μM DA in PBS, for both MPA and control sensors. The signal drift was calculated with a linear fit between 110 s and 600 s. The MPA effect on the signal drift was evaluated by comparing the slopes from the linear fits, see Table below for details.

Table S1. Results of the signal drift calculation from the 10-minutes redox cycling experiment. The linear fit results were averaged ($n = 2$) and are displayed in the table with the correlated standard error and the slope in degrees. The effect of MPA at the generator removed the signal drift (the value marked with an asterisk was not significantly different from zero). The MPA effect on the collector (cathodic currents) significantly reduced drift of signal from a positive (decreasing signal) slope to a slightly negative value (increasing signal over time), overall this shows a positive impact of MPA on the signal stability.

	Angular coefficient from linear fit Mean ($n = 2$) (nA/s)	Standard Error for angular coefficient (nA/s)	Slope (degrees)	t-test on slope values (one-tailed) Mean ($n = 2$)
Generator Control	-0.0678	8.23 E-05	-3.88	Generator Control vs Generator MPA: $p < 0.01$
Generator MPA	* -2 E-05	2.15 E-05	* -0.0011	
Collector MPA	-0.00903	1.02 E-04	-0.518	Collector Control vs Collector MPA $p < 0.01$
Collector Control	0.0497	1.11 E-04	2.85	

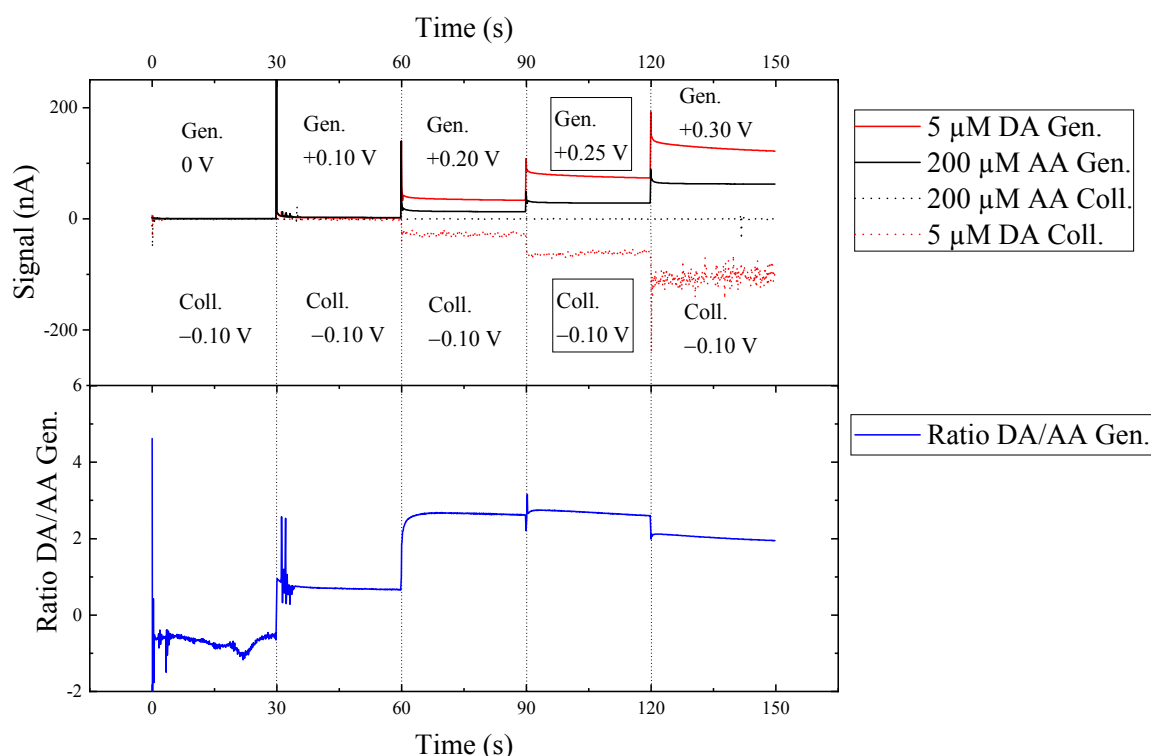


Figure S2. Optimization of the generator potential. On the top: Chronoamperometric responses of DA and AA at the sensor with increasing generator electrode potentials. The potential was stepped every 30 s from 0 to +0.30 V, the collector potential was set to -0.1 V. On the bottom: ratio of the recorded DA and AA signals. The experiment was performed in PBS (pH = 7.4)

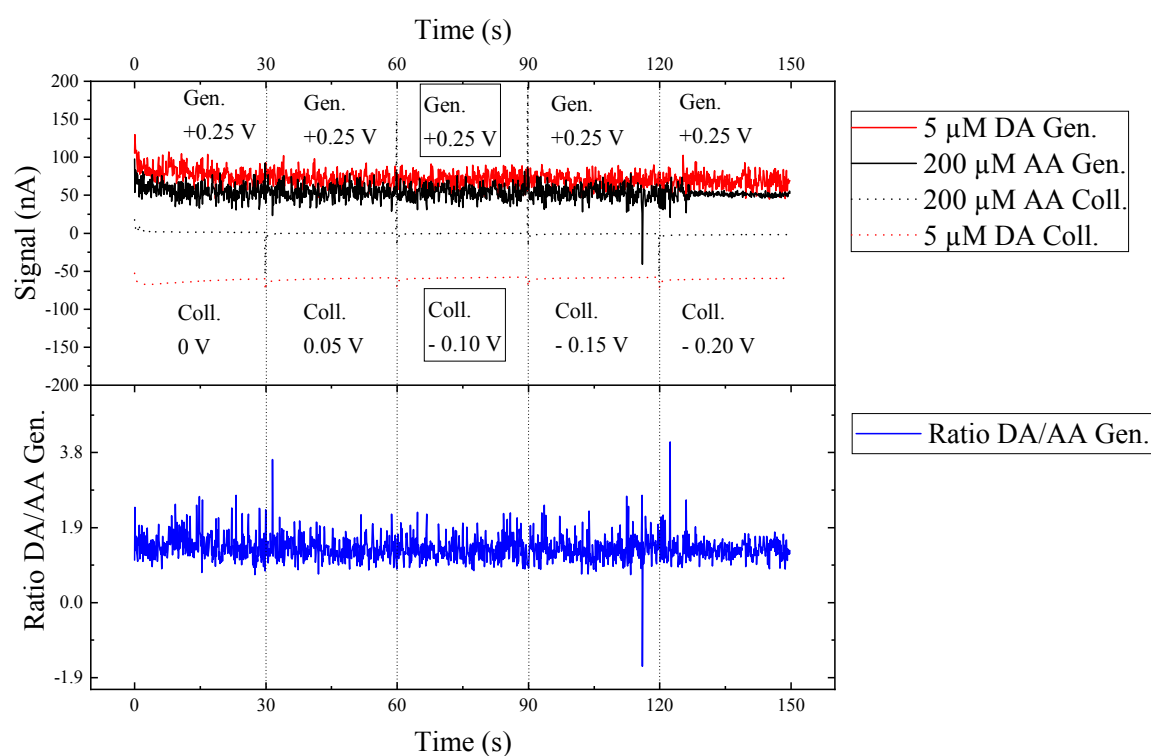


Figure S3. Optimization of the collector potential. On the top: chronoamperometric responses of DA and AA at the sensor with decreasing collector electrode potentials. The potential was stepped every 30 s from 0 to -0.20 V, the generator potential was set to +0.25 V. On the bottom: ratio of the recorded DA and AA signals. The experiment was performed in PBS (pH = 7.4).

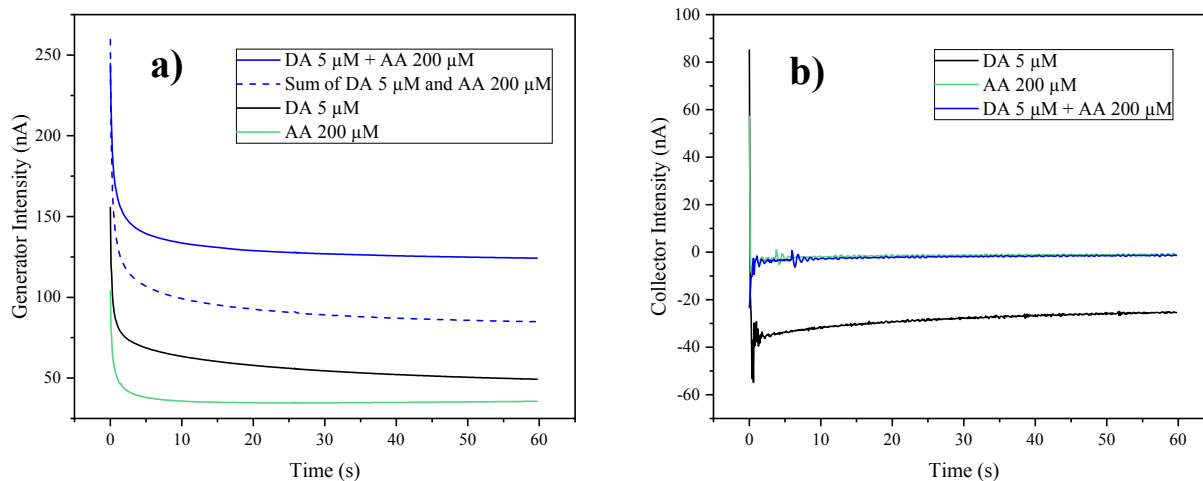


Figure S4. Generator and Collector signals of ascorbic acid (AA) and dopamine (DA) solutions in PBS at MPA modified sensor. a) At the generator the DA signal is higher than the AA signal, and when the two components are mixed in the same solution the resulting signal is higher than the sum of the separate ones, this synergic action is attributed to AA reducing DA-quinone, thus increasing diffusion gradients and leading to higher currents; b) at the collector the AA signal is silent, while the DA signal is visible (due to reduction of DA-quinone), the copresence of DA and AA in solution leads to a silent signal, this is also attributed to AA reducing DA-quinone.

Table S2. Sensor intra-batch and inter-batch repeatability. Each sensitivity measurement was obtained from the slope of a 0-1000 nM DA calibration curve in PBS.

Replicate Batch	DA sensitivity (nC/nM)				Intra-batch CV (<i>n</i> = 4)	Inter-batch CV (<i>n</i> = 3)
	1	2	3	4		
A	0.955	0.973	0.960	1.041	4.1 %	9.9 %
B	1.113	1.084	1.090	1.085	1.3 %	
C	1.240	1.171	1.259	1.242	3.2 %	

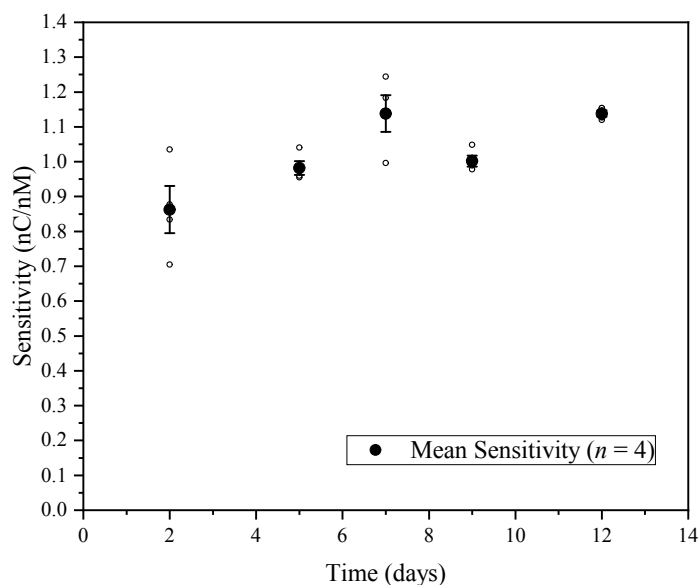


Figure S5. Time resolved monitoring of DA sensitivity of the sensor (*n* = 4) to assess sensor stability. The slope of the linear regression was not significantly different from zero ($\alpha = 0.05$).

Table S3. Long-term stability study. DA signal was measured on the month of manufacturing and also after 20 months (*n* = 3). Selectivity towards AA was also measured after 20 months.

replicate	DA signal (nC/nM) at month 0	DA signal (nC/nM) at month 20	% change	Selectivity towards AA after 20 months
A	0.86	0.41	-52 %	57
B	0.58	0.53	-8%	49
C	0.76	0.52	-31%	68
Average \pm SD	0.73 \pm 0.14	0.49 \pm 0.07	-33 \pm 22 %	58 \pm 9.5

Table S4. Detailed Results of the analysis of selectivities to DA change after MPA modification. The selectivity was calculated as the ratio of the biomolecule signal (nC/nM) and the DA signal (nC/nM). The percent change represents the change in selectivity to DA after MPA modification. Not detected or n.a.: the signal of the compound was not significantly different from the background (PBS, $\alpha = 0.05$, two-tailed t test).

Selectivity to DA (standard deviation, $n = 3$) at the control sensor and at MPA modified sensor, percent change after MPA modification.						
	Generator			Collector		
Compound	Control	MPA	% Change	Control	MPA	% Change
Norepinephrine	1.8 (0.02)	1.9 (0.05)	+4%	2.9 (0.02)	3.7 (0.02)	+30%
L-DOPA	3 (0.02)	15.8 (0.04)	+419%	8.2 (0.02)	Not detected	n.a.
Epinephrine	3.5 (0.03)	2.2 (0.04)	-37%	83.7 (0.02)	Not detected	n.a.
AA	6.9 (0.02)	55 (0.04)	+702%	3714.6 (0.02)	Not detected	n.a.
DOPAC	11.1 (0.02)	115.2 (0.04)	+934%	11.4 (0.02)	Not detected	n.a.
GABA	288 (0.02)	Not detected	n.a.	Not detected	Not detected	n.a.

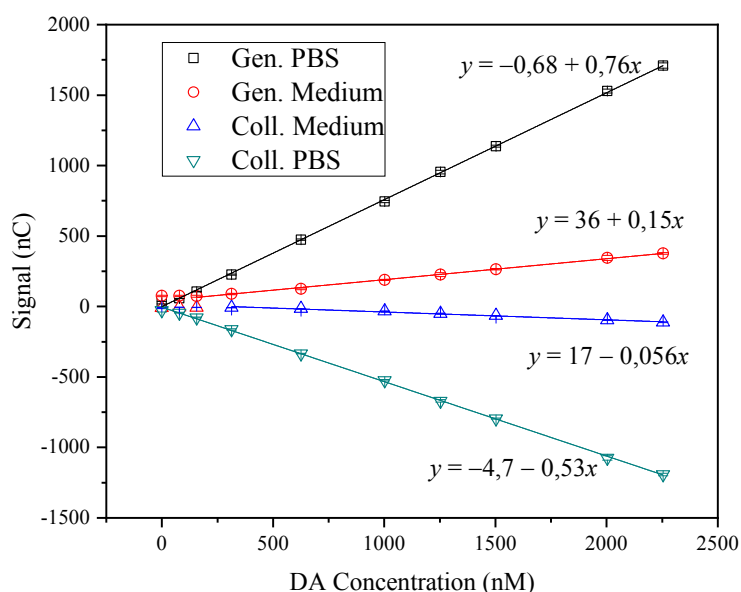


Figure S6. Electrochemical sensor calibration of DA in both PBS and cell culture medium. Generator (Gen.) signals include PBS (open squares) and cell culture medium (open circles). Collector (Coll.) signals include PBS (up open triangles) and cell culture medium (down open triangles). Linear regressions equations are visible. Error bars: standard error of the mean.

Table S5. Detailed results of the linear regression of DA calibration in PBS and cell culture medium. The LOD was calculated as the value of the blank (cultivated cell culture medium) plus three times the error of the blank (SEM). The lowest limit of the linear range is the adjusted to be \geq LOD.

Signal, Solvent	LOD	Linear Range	Intercept		Slope		Statistics
	Value \pm C.I. $\alpha = 0.05$ (nM)	Concentration (nM)	Value (nC)	Standard Error	Value (nC/nM)	Standard Error	Adj. R-Square
Generator, PBS	69 \pm 25	157–2254	-0.68	6.37	0.759	0.005	0.99956
Generator, Medium	369 \pm 44	369–2254	41.71	3.74	0.149	0.003	0.99755
Collector, Medium	476 \pm 249	476–2254	16.75	3.82	-0.056	0.003	0.9864
Collector, PBS	108 \pm 29	108–2254	-4.68	5.21	-0.528	0.004	0.99939

LC-MRM-MS

Table S6. Elution program of the LC-MRM-MS method using 0.1 % aqueous formic acid as eluent A and acetonitrile as eluent B.

Time (min)	B %	Flow rate (ml/min)
0	2	0.4
4	2	0.4
8	80	0.4
9	90	0.4
10	2	0.4
12	2	0.4

Table S7. Ion transitions relevant for the established LC-MRM-MS method to detect and quantify six biomolecules and the internal standard.

Analyte	Retention time (min)	MRM Transitions (precursor ion mass > product ion mass)		
		quantitation	confirmation	
GABA	1.2	104.30 > 87.15	104.30 > 45.10	104.30 > 69.05
Norepinephrine	1.4	170.10 > 135.10	170.10 > 107.10	170.10 > 152.20
Epinephrine	1.8	184.10 > 166.20	184.10 > 123.10	184.10 > 107.10
d3-L-DOPA	2.0	201.10 > 110.20	201.10 > 154.75	201.10 > 184.30
L-DOPA	2.0	198.20 > 152.15	198.20 > 107.10	198.20 > 181.15
Dopamine	2.1	154.10 > 137.00	154.10 > 119.10	154.10 > 91.00
DOPAC	6.2	166.80 > 123.05	166.80 > 122.85	166.80 > 105.00

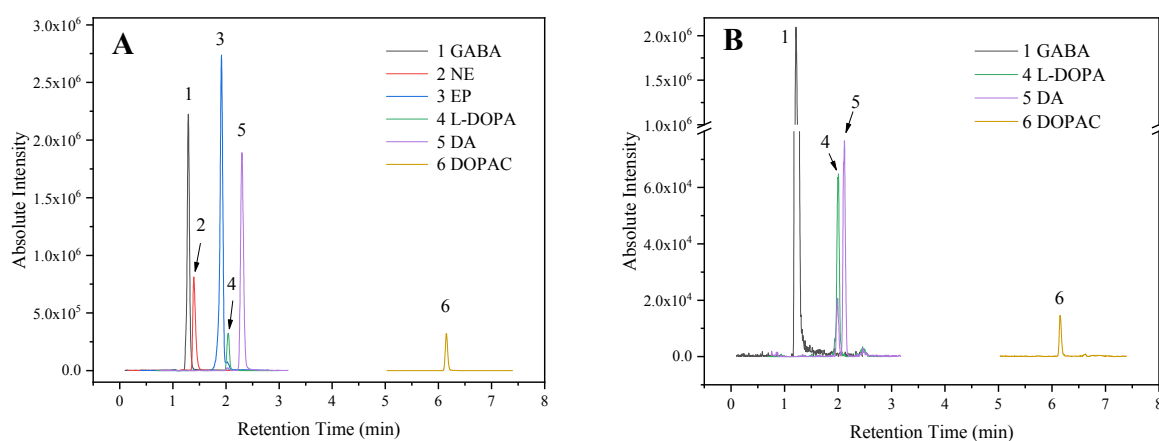


Figure S7. LC-MRM-MS chromatograms showing chromatographic performance for the most intense MRM transitions. A) Injection of an aqueous mixture of standards (on column: 19.3 pmol GABA, 2.5 pmol norepinephrine (NE), 3.1 pmol epinephrine (EP), 3.7 pmol L-DOPA, 4.0 pmol dopamine (DA), 9.1 pmol DOPAC); B) Chromatogram of the healthy organoid line sample at day 60. EP and NEP had a S/N < 3.

Table S8. Limits of Detection (LOD) and Limits of Quantitation (LOQ) obtained for 6 neurotransmitters measured from cell culture medium after minimal sample preparation by LC-MRM-MS. 5 μ l injections. LOD: S/N > 3, LOQ: S/N > 10.

	LOD (nM)	LOQ (nM)
GABA	4.3	14.2
Norepinephrine	8.6	28.8
Epinephrine	2.5	8.3
L-DOPA	13.5	44.9
Dopamine	10.9	36.2
DOPAC	12.4	41.4

Table S9. Summary of intraday reproducibility for the LC-MRM-MS analysis of neurotransmitters measured directly from cell culture medium after minimal sample preparation. On the left column averaged coefficient of variation (CV) values of four different human midbrain organoid supernatant (differentiation day 60), N/A: data not available (S/N < 3); On the right column averaged CV values of five different standard dilutions (S/N > 10, same data as Table 3 in the manuscript). Every injection was done thrice.

	% Intraday CV samples (<i>n</i> = 4, triplicate inj.)	% Intraday CV standards (<i>n</i> = 5, triplicate inj.)
GABA	6.5	10.5
Norepinephrine	N/A	4.3
Epinephrine	N/A	8.7
L-DOPA	5.6	3.1
Dopamine	3.8	14.6
DOPAC	5.2	3.0

Cell Culture and Immunohistochemistry

Table S10. hMO lines description with references.

Line name in this work	CRISPR/Cas9	LRRK2 gene	Line name in ref.	Reference
Healthy	No	WT	Healthy2	Qing et al., 2017
Healthy-Mut	Yes	G2019S	Healthy2-Mut	Qing et al., 2017
PD1	No	G2019S	PD1	Reinhardt et al., 2013
PD2	No	G2019S	PD2	Reinhardt et al., 2013
PD2-GC	Yes	WT	PD2-GC	Reinhardt et al., 2013

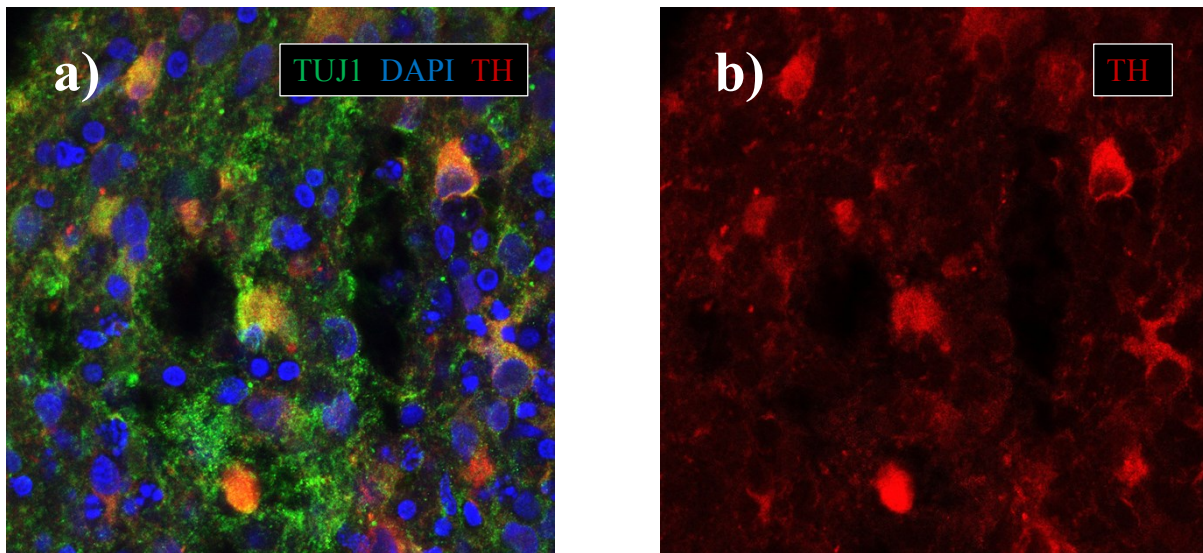


Figure S8. Immunohistochemical staining of an hMO at day 53 of differentiation. The staining reveals tyrosine hydroxylase (TH, red) positive dopaminergic neurons ((a) and (b)) as well as the neuronal marker TUJ1 (green) and DAPI stained nuclei (blue) (a).